

CRISPR-Cas9-Mediated Genome Editing Increases Lifespan and Improves Motor Deficits in a Huntington's Disease Mouse Model

Freja K. Ekman,¹ David S. Ojala,² Maroof M. Adil,² Paola A. Lopez,³ David V. Schaffer,^{2,3,4,5} and Thomas Gaj^{6,7}

¹Department of Chemistry, University of California, Berkeley, Berkeley, CA, USA; ²Department of Chemical and Biomolecular Engineering, University of California, Berkeley, Berkeley, CA, USA; ³Department of Bioengineering, University of California, Berkeley, Berkeley, CA, USA; ⁴Department of Molecular and Cell Biology, University of California, Berkeley, Berkeley, CA, USA; ⁵The Helen Wills Neuroscience Institute, University of California, Berkeley, Berkeley, CA, USA; ⁶Department of Bioengineering, University of Illinois, Urbana, IL, USA; ⁷Carl R. Woese Institute for Genomic Biology, University of Illinois, Urbana, IL, USA

Huntington's disease (HD) is a currently incurable and, ultimately, fatal neurodegenerative disorder caused by a CAG trinucleotide repeat expansion within exon 1 of the huntingtin (HTT) gene, which results in the production of a mutant protein that forms inclusions and selectively destroys neurons in the striatum and other adjacent structures. The RNA-guided Cas9 endonuclease from CRISPR-Cas9 systems is a versatile technology for inducing DNA double-strand breaks that can stimulate the introduction of frameshift-inducing mutations and permanently disable mutant gene function. Here, we show that the Cas9 nuclease from *Staphylococcus aureus*, a small Cas9 ortholog that can be packaged alongside a single guide RNA into a single adeno-associated virus (AAV) vector, can be used to disrupt the expression of the mutant HTT gene in the R6/2 mouse model of HD following its *in vivo* delivery to the striatum. Specifically, we found that CRISPR-Cas9-mediated disruption of the mutant HTT gene resulted in a ~50% decrease in neuronal inclusions and significantly improved lifespan and certain motor deficits. These results thus illustrate the potential for CRISPR-Cas9 technology to treat HD and other autosomal dominant neurodegenerative disorders caused by a trinucleotide repeat expansion via *in vivo* genome editing.

INTRODUCTION

Huntington's disease (HD) is an autosomal dominant neurodegenerative disorder characterized by a progressive decline in cognitive, motor, and psychiatric function.¹ HD is the most common inherited neurodegenerative disease, affecting ~1 in 10,000 individuals, and is caused by the expansion of a CAG trinucleotide repeat within exon 1 of the huntingtin (HTT) gene.² The presence of this expansion leads to the production of a mutant protein that aggregates in the brain and disrupts important cellular functions,^{3,4} such as nucleocytoplasmic transport,⁵ which primarily results in the loss of medium-sized spiny neurons (MSNs) and certain cortical neurons that project to the striatum.^{6–8} Most individuals with HD first experience disease-associated abnormalities between 35 and 45 years of age and typically perish from the disorder ~20 years after its manifestation.⁹ There is

no cure for HD, and currently approved therapies can only help to manage certain physical and psychiatric symptoms.¹⁰

Although the exact mechanism by which the mutant HTT protein destroys neurons remains unknown, multiple lines of evidence have suggested that deleting or reducing mutant HTT gene expression within affected areas of the brain can halt the progression of HD.^{11,12} Accordingly, both antisense oligonucleotides (ASOs) and RNAi have been used to reduce mutant HTT and improve behavioral deficits in transgenic animal models of the disorder.^{13–19} In fact, a phase I clinical trial designed to assess the safety and tolerability of ASOs targeting SNPs associated with the mutant CAG repeat expansion (ClinicalTrials.gov: NCT03225833 and NCT03225846) is underway. Additionally, a clinical trial involving an ASO targeting both mutant and wild-type HTT mRNAs has yielded early encouraging results (ClinicalTrials.gov: NCT02519036), indicating that targeting both the native and the mutant HTT proteins could be tolerated in a clinical setting. Further, a microRNA-based gene therapy for HD^{20–22} is in the final stages of pre-clinical development and could soon be evaluated in patients. However, despite advances in chemistry and design, ASOs can only transiently repress the production of the HTT protein and may still require a lifetime of administrations to patients, while RNAi is prone to off-target effects.^{23–25} Additionally, both ASOs and RNAi are associated with incomplete knockdown and lack the capacity to correct the underlying genetic defect responsible for HD, which could ultimately limit their utility as therapeutics.

Genome editing—a method that enables the precise alteration of a targeted DNA sequence—offers an alternative approach to treat HD by providing a means to permanently disrupt the function of

Received 12 December 2018; accepted 16 July 2019;
<https://doi.org/10.1016/j.omtn.2019.07.009>.

Correspondence: David V. Schaffer, Department of Chemical and Biomolecular Engineering, University of California, Berkeley, Berkeley, CA, USA.
E-mail: schaffer@berkeley.edu

Correspondence: Thomas Gaj, Department of Bioengineering, University of Illinois, Urbana, IL, USA.
E-mail: gaj@illinois.edu



the HTT gene.²⁶ CRISPR (clustered regularly interspaced short palindromic repeats)-CRISPR-associated (Cas) systems,^{27–31} in particular, have emerged as especially versatile and efficient gene-editing technologies that hold considerable potential as therapeutics.³² The CRISPR-Cas9 DNA-editing system consists of two core components: the Cas9 nuclease and a single guide RNA (sgRNA) that binds to Cas9 and directs it to a targeted genomic site via RNA-DNA base complementarity.²⁷ Upon DNA binding, Cas9 introduces a DNA double-strand break (DSB) that stimulates non-homologous end joining (NHEJ), an error-prone DNA repair pathway that facilitates the introduction of random base insertions and deletions (indels) that can lead to a frameshift mutation³³ and thereby disrupt gene expression via nonsense-mediated mRNA decay.³⁴ As a result, CRISPR-Cas9 technology could be used to disable the production of the HTT protein and treat HD following its *in vivo* delivery to areas of the brain most affected by the disorder.

In the present study, we demonstrate that CRISPR-Cas9 can be deployed to the striatum via a single adeno-associated virus (AAV) vector particle to disable the expression of the human mutant HTT gene in an especially aggressive animal model of the disorder. Specifically, we show that CRISPR-Cas9-mediated disruption of the mutant HTT gene in R6/2 mice, which carry exon 1 of the human HTT gene with ~115–150 CAG repeats, reduces the formation of neurotoxic inclusions by 2-fold, increases lifespan, and improves certain motor deficits in these same mice. Our results illustrate the potential for CRISPR-Cas9 technology to treat HD and reinforce its potential for treating other autosomal dominant neurodegenerative disorders.

RESULTS

Using CRISPR-Cas9 to Disrupt HTT Gene Expression

Owing to its ability to induce targeted DSBs that can drive the formation of frameshift-inducing indels, we hypothesized that CRISPR-Cas9 could be used to disrupt the expression of the HTT gene following its *in vivo* delivery using an AAV vector, a clinically promising engineered gene delivery vehicle^{35,36} capable of transducing various substructures within the brain,³⁷ including the striatum. AAV vectors, however, have a limited carrying capacity that restricts single-particle delivery of the prototypical Cas9 nuclease from *Streptococcus pyogenes* (SpCas9) alongside an sgRNA expression cassette.³⁸ Thus, in order to more effectively deliver a CRISPR-Cas9 gene-editing system *in vivo*, we used the Cas9 nuclease from *Staphylococcus aureus* (SaCas9) to target the human HTT gene.³⁹ SaCas9 is ~1 kb smaller than SpCas9 and can fit into a single AAV particle along with an sgRNA and a neuron-specific promoter to drive its expression *in vivo*.

We designed several sgRNAs to target exon 1 of the human HTT gene either upstream or downstream of the CAG repeat expansion, with the expectation that SaCas9-induced indels would reduce the production of the human HTT protein (Figure 1A). Given that the CAG trinucleotide repeat, as well as the large size of the full-length HTT protein (~350 kDa) can confound quantitative analyses, we used an established reporter that inducibly expresses exon 1 of the human

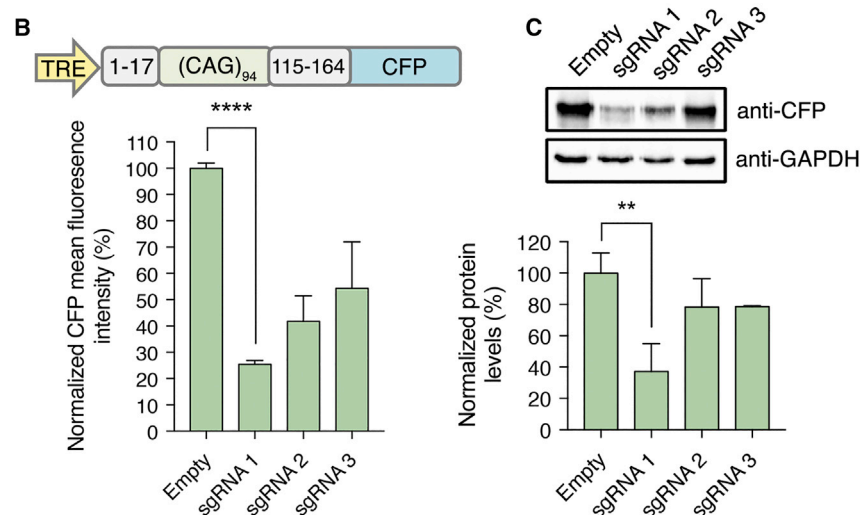
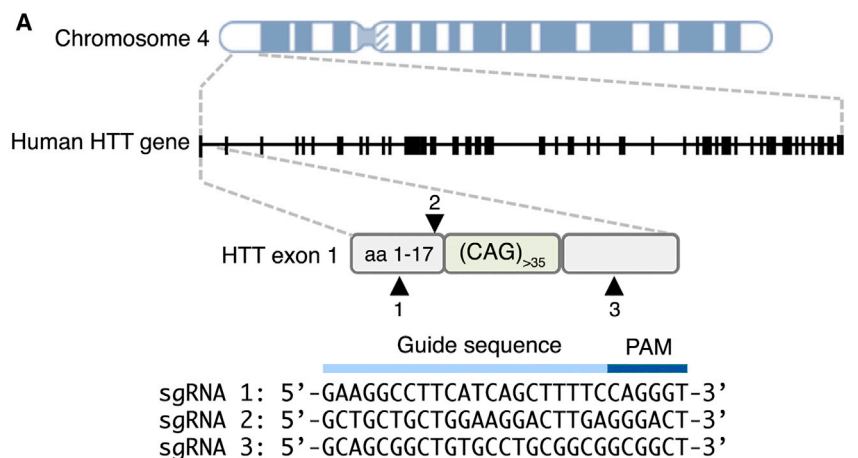
HTT gene with 94 glutamines (94Q) fused to a cyan fluorescent protein (CFP) variant (Figure 1B),⁴⁰ thereby linking mutant HTT gene expression to CFP fluorescence for facile evaluation of the designed sgRNAs. Following transfection into HEK293T cells, we observed that each sgRNA decreased CFP fluorescence intensity by at least 50%, with the most effective sgRNA reducing fluorescence by ~75% ($p < 0.007$) (Figure 1B). These findings were corroborated by western blot, which indicated a ~65% decrease in mutant HTT-CFP fusion protein for the most efficient sgRNA in comparison to control cells ($p < 0.0001$) (Figure 1C). Sanger sequencing further confirmed the presence of SaCas9-induced indels for this sgRNA within the mutant HTT transgene, though we identified mutations in only ~10% of sequenced amplicons (Figure S1). Given the proximity of the sgRNA target site to the 3' primer binding site used for this PCR amplification, we anticipate that SaCas9 could have mutated a fraction of these sites, thereby preventing efficient amplification of a subset of the edited transgenes. Collectively, these results indicate that SaCas9 can be used to target the human HTT gene and reduce mutant HTT protein in reporter cells.

CRISPR-Cas9 Reduces Mutant HTT Protein Inclusions in the R6/2 Mouse Model of HD

We next evaluated whether the SaCas9 nuclease could reduce mutant HTT protein *in vivo* following its delivery to the R6/2 mouse model of HD, a transgenic mouse strain that carries the 5' end of the human HTT gene, which includes: (1) ~1 kb of the 5' UTR sequence, (2) exon 1 of the HTT gene with ~115–150 CAG repeats, (3) the first 262 bp of intron 1, and (4) a 168-bp foreign segment from bacterial DNA^{41,42} (Figure 2A). R6/2 mice develop HTT protein inclusions in the striatum and, eventually, the cortex and exhibit a progressive neurodegenerative phenotype that mimics many features of HD in humans, including weight loss, tremors, epileptic seizures, movement abnormalities, and premature death.^{43,44} This strain is a well-characterized and a widely used model for studying and evaluating potential treatments for HD.

We injected the striatum of 4-week-old R6/2 mice at three depths with 2×10^{10} viral genomes (vg) of an AAV1 vector encoding SaCas9 and either the most efficient sgRNA targeting the human HTT gene (AAV1-SaCas9-HTT) or an sgRNA targeting the mouse Rosa26 locus (AAV1-SaCas9-mRosa26), a safe harbor site that can support stable transgene expression.⁴⁵ Transgenic mice injected with AAV1-SaCas9-mRosa26 previously showed no signs of toxicity and displayed no changes in disease progression compared to those injected with an EGFP-encoding AAV,⁴⁶ indicating the suitability of AAV1-SaCas9-mRosa26 as a negative control. Additionally, AAV1 can effectively transduce neurons in the striatum⁴⁷ and has previously been used to deliver neurotrophic factors⁴⁸ and engineered RNAi systems⁴⁹ to HD rodent models. To ensure that SaCas9 is specifically expressed in neurons, we used the human synapsin (hSyn) promoter to drive its expression from the AAV vector (Figure 2B).

Four weeks after AAV delivery (Figure 2C), we used immunohistochemistry (IHC) to analyze brain sections from treated and untreated animals for the expression of: (1) SaCas9 via its



hemagglutinin (HA) epitope tag; (2) MSNs, the major neuronal cell type of the striatum, using an antibody that targets the MSN-specific marker DARPP-32; and (3) mutant HTT, using an antibody that has been reported to efficiently recognize the mutant form of the human protein⁵⁰ (Figure 2D). We observed SaCas9 expression in the central striatum (Figure S2), with quantitative analysis revealing that ~85% of DARPP-32⁺ cells in the injected area expressed SaCas9 (Figure S3). Importantly, we also found that R6/2 mice infused with AAV1-SaCas9-HTT had ~40% fewer mutant HTT protein inclusions in dual SaCas9⁺ and DARPP-32⁺ cells compared to animals injected with AAV1-SaCas9-mRosa26 ($p = 0.003$) (Figure 2E). Western blot analysis further revealed that mice treated by CRISPR-Cas9 had ~50% less total mutant HTT protein in whole striatal lysate compared to control animals ($p < 0.008$) (Figure 2F; Figure S4).

To evaluate whether SaCas9 induced indels *in vivo*, we deep sequenced the human HTT transgene from whole dissociated striatal tissue, which consisted of a mixture of transduced and non-

Figure 1. Disruption of the Mutant HTT Gene in Reporter Cells Using CRISPR-Cas9 Nucleases

(A) Schematic representation of the human HTT locus located on chromosome 4 and the candidate sgRNA target sites. Arrowheads indicate the approximate location of the sgRNA binding site. aa, amino acids; PAM, protospacer-adjacent motif. (B) Top: graphic of the mutant HTT-CFP reporter. Bottom: the percentage of CFP-positive HEK293T cells 72 h after transfection with reporter plasmid, SaCas9, and the HTT-targeting sgRNAs or a non-targeted sgRNA (Empty) ($n = 3$). (C) Top: western blot of lysate from HEK293T cells 72 h after transfection with reporter plasmid, SaCas9, and the HTT-targeting sgRNAs or a non-targeted sgRNA (Empty). Bottom: quantitation of western blot results. CFP protein was normalized to GAPDH protein in each lane ($n = 3$). Error bars indicate SD. ** $p < 0.01$; *** $p < 0.001$, unpaired t test.

transduced cells. According to CRISPResso,⁵¹ a computational pipeline for quantifying genome-editing outcomes from sequencing data, indels were present in ~6% of the analyzed human HTT transgenes from CRISPR-treated animals, which corresponded to a ~12-fold increase in indels compared to that in control mice, though we observed indel frequencies up to 14% in some animals (Figure S5). To determine whether SaCas9 induced off-target effects, we deep sequenced 10 candidate off-target sites identified using the web-based tool Cas-OFFinder.⁵² CRISPResso analysis revealed no increase in indel formation at any of the 10 sites, including the mouse HTT gene, which deviates from the human sgRNA target site by 1 bp (Figure S6). Taken together, these results indicate that SaCas9-mediated disruption of the mutant HTT gene can reduce mutant protein in the brain.

CRISPR-Cas9-Mediated Disruption of the Mutant HTT gene Increases Survival in R6/2 Mice

We next sought to determine whether CRISPR-Cas9-mediated disruption of the mutant HTT gene could provide therapeutic benefit to R6/2 mice, which develop a particularly aggressive and rapid form of neurodegeneration and have a shortened lifespan (typically, 16 weeks of age) compared to other transgenic models of the disorder. Starting at 4 weeks after AAV injections, we measured motor function, hindlimb clasping (an established indicator of dystonia, a clinical characteristic of HD), and weight on a weekly basis, with end-stage determined as the point at which animals either were moribund, lacked a righting reflex, or failed to respond to gentle stimulation.

R6/2 mice injected with AAV1-SaCas9-HTT displayed a ~15% increase in mean survival compared to control animals (HTT: 95.4 ± 2.5 days; mRosa26: 82.8 ± 3.7 days; $p < 0.01$) (Figure 3A) and had

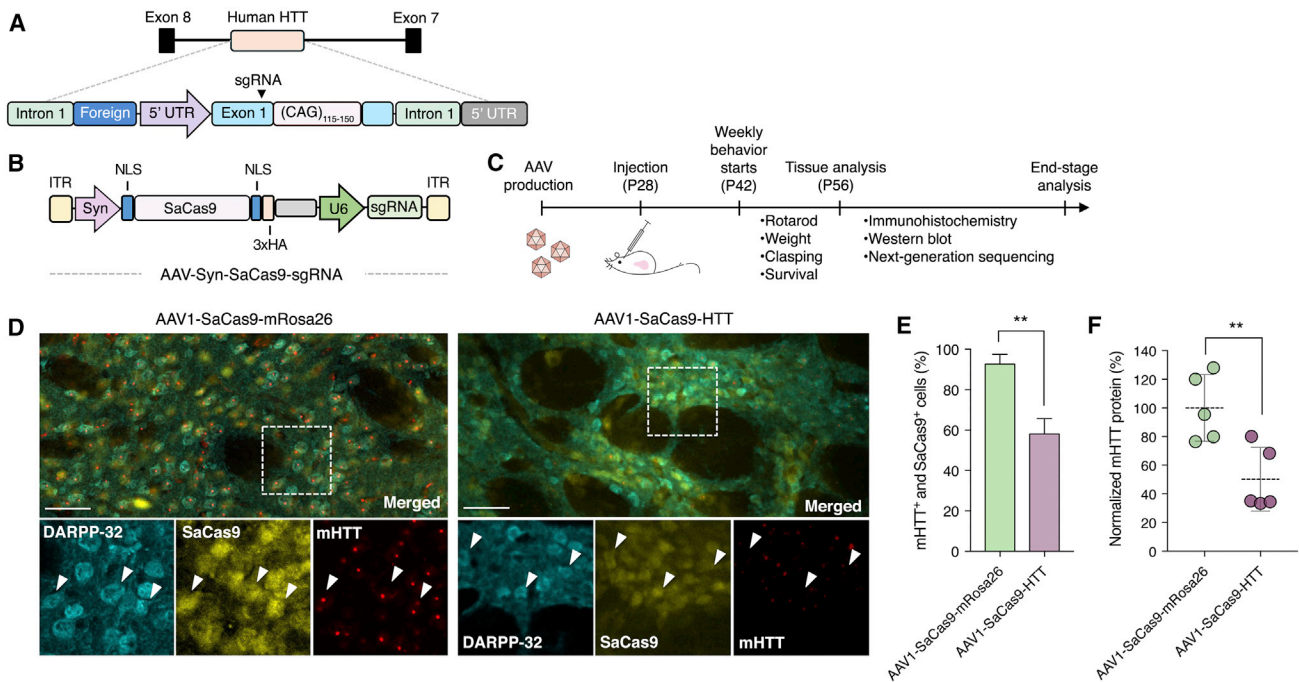


Figure 2. In Vivo Disruption of the Mutant HTT Gene in R6/2 Mice

(A) Cartoon of the human HTT transgene located in *Gm12695* (predicted gene 12695) on chromosome 4 in R6/2 mice. Arrowhead indicates approximate location of sgRNA binding site. (B) Schematic of the AAV vector. ITR, inverted terminal repeat; hSyn, human synapsin promoter; NLS, nuclear localization sequence; 3xHA, three tandem repeats of the human influenza hemagglutinin (HA) epitope tag. (C) Timeline for *in vivo* studies. (D) Immunofluorescent staining of striatal sections 4 weeks after R6/2 mice were injected with 6×10^{10} vector genomes of (left) AAV1-SaCas9-mRosa26 or (right) AAV1-SaCas9-HTT. Insets show high-magnification images. Arrowheads indicate representative DARPP-32⁺ and SaCas9⁺ cells with (left) high or (right) reduced mutant HTT (mHTT) protein. Images were captured using identical exposure conditions. Scale bars, 50 μ m. (E) Quantitation of immunohistochemical results from R6/2 mice injected with AAV1-SaCas9-HTT ($n = 3$) or AAV1-SaCas9-mRosa26 ($n = 3$). (F) Normalized mutant HTT protein in striatal lysate 4 weeks after R6/2 mice were injected with 6×10^{10} vg of AAV1-SaCas9-mRosa26 or AAV1-SaCas9-HTT ($n = 5$). ** $p < 0.01$, unpaired *t* test. Error bars indicate SD. All injections were performed on 28-day-old animals.

lifespans that ranged from 80 to 106 days, compared to 66 to 98 days for control mice ($p = 0.01$) (Figure 3B). We also observed that R6/2 mice treated by SaCas9 gene editing had improved motor function ($p < 0.01$) (Figure 3C) and decreased hindlimb claspings at multiple weeks, including week 12 ($p < 0.05$), week 13 ($p < 0.01$), and week 14 ($p = 0.05$) (Figure 3D). In fact, we observed that more than half of all treated animals did not exhibit any signs of claspings until week 11, whereas 80% of the AAV1-SaCas9-mRosa26-treated animals had clasped by week 10. Interestingly, we observed no difference in weight (typically an indicator of disease onset) between treated and untreated mice (Figure S7), which could be due to the fact that, while HTT protein inclusions can develop as early as 2 weeks of age in R6/2 mice,^{53,54} we injected AAV vector into 4-week-old animals. Thus, earlier administration of the AAV vector to this strain or delivery to a late-onset model of HD⁵⁵ could shed more light on the ability of SaCas9 to slow the onset of the disease.

Finally, immunohistochemical analysis of striatal sections from both treated and untreated animals at end-stage revealed that gene-edited mice had $\sim 30\%$ fewer mutant HTT protein inclusions in SaCas9⁺ cells compared to control animals ($p < 0.05$) (Figures 4A and 4B).

Additionally, we found that end-stage mice had $\sim 10\%$ more total SaCas9⁺ cells than animals infused with AAV1-SaCas9-mRosa26 (Figure S8). Since we observed similar transduction efficiency in animals injected with AAV1-SaCas9-HTT and AAV1-SaCas9-mRosa26 (Figure S2), these results likely indicate that CRISPR-mediated disruption of the mutant HTT gene can impart protection to some neurons from mutant HTT-induced toxicity.

Collectively, these results establish that CRISPR-Cas9 can be used to reduce mutant HTT protein in R6/2 mice and that SaCas9-mediated disruption of the mutant HTT gene can significantly increase survival and improve motor deficits.

DISCUSSION

HD is the most common inherited neurodegenerative disorder, affecting over 30,000 people in the United States,⁵⁶ with an estimated 200,000 individuals at risk of inheriting the disease in the United States alone. There is no cure for HD, and current therapies only provide symptomatic relief. Thus, there is an urgent need for strategies that can reduce the formation of toxic HTT protein inclusions and treat the underlying cause of the disorder. Here, we show that CRISPR-Cas9—a versatile

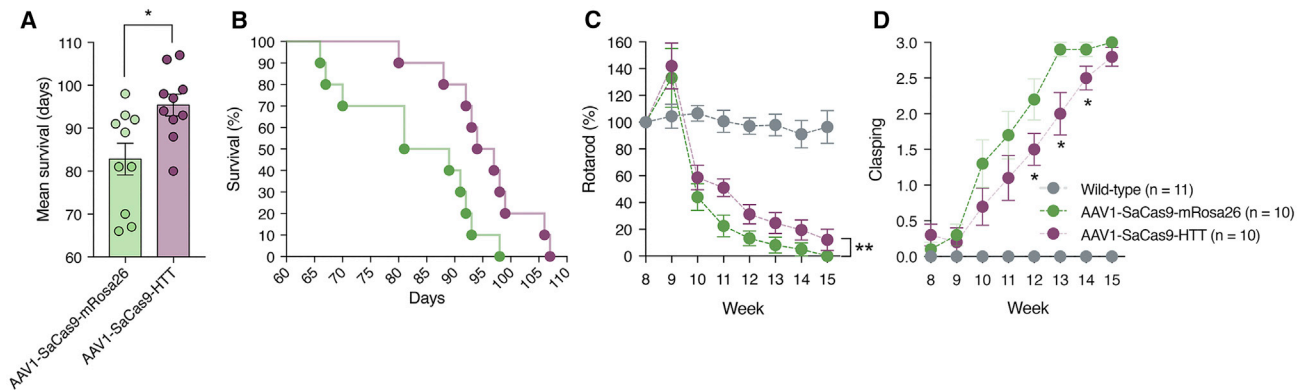


Figure 3. CRISPR-Cas9-Mediated Disruption of the Mutant HTT Gene Provides Therapeutic Benefit to R6/2 Mice

(A–D) Mean survival (A), percent survival (B), normalized rotarod (C), and normalized clasping (D) scores for R6/2 mice bilaterally injected with 6×10^{10} vg of AAV1-SaCas9-HTT ($n = 10$) and AAV1-SaCas9-mRosa26 ($n = 10$). Wild-type mice ($n = 11$) are litter-matching B6CBAF1 mice. Values are means, and error bars indicate SEM. * $p < 0.05$. In (B), unpaired t test was used; in (C) and (D), a two-way ANOVA was used, followed by Tukey's post hoc analysis.

technology that we^{46,57} and others^{58–62} have established can be deployed in the nervous system to facilitate genome editing—can be harnessed to disrupt the expression of the mutant HTT gene in the R6/2 mouse model of HD, one of the most aggressive transgenic animal models of the disorder.⁶³ Specifically, we demonstrate that CRISPR-Cas9 can be used to reduce neuronal protein inclusions following its delivery to the striatum, an outcome that resulted in increased lifespan and improved motor function. Our study thus illustrates the potential for genome editing to treat HD.

Since R6/2 mice harbor the 5' end of exon 1 of the human HTT gene with an expansion of ~ 115 – 150 CAG trinucleotide repeats, we designed sgRNAs to target exon 1 of the human HTT allele. As a result, this therapeutic genome-editing strategy is not allele specific and unable to discriminate between the mutant and wild-type forms of the HTT gene in an HD patient. However, while disrupting the wild-type HTT gene can affect early neurological development and lead to embryonic lethality or cause certain side effects in young mice,^{64–66} several studies have suggested that reducing wild-type and mutant HTT protein in adult mice^{18,66} and larger animals²¹ is well tolerated. In fact, a clinical trial aimed at accessing the safety of an ASOs targeting both the mutant and wild-type HTT mRNA is underway (ClinicalTrials.gov: NCT02519036), with more in the pipeline,^{20–22} underscoring the therapeutic feasibility of a non-allele-specific targeting approach, though additional studies are still needed to firmly establish this. In the case that specific disruption of the mutant HTT gene is required, CRISPR-Cas9 could be deployed to target distinct heterozygous SNPs associated with the CAG repeat, which was demonstrated as feasible in previous studies.^{16,19,60} However, since many of these SNPs vary among the patient population, this approach would likely require using different specialized CRISPR-Cas9 systems to target each mutation, which could make its implementation challenging.

To date, several genome-editing and targeted gene-regulating technologies have been used to reduce the expression of the mutant

HTT gene, including an engineered zinc-finger repressor protein that targeted the CAG repeat expansion⁶⁷ and also CRISPR-Cas9, which has been used to excise an expanded CAG repeat⁵⁹ and disrupt the expression of the HTT gene.^{60,61} However, to our knowledge, no other study has demonstrated that CRISPR-Cas9 technology can increase survival in an HD animal model, an important benchmark for a HD therapeutic. In particular, while Yang et al.⁵⁹ used the SpCas9 nuclease to delete the CAG repeat expansion in HD140Q-knockin mice (which express exon 1 of the human mutant HTT gene in place of exon 1 of the mouse HTT gene), they did not analyze survival and reported that only early neuropathology effects were attenuated by gene editing. Similarly, while Monteys et al.⁶⁰ reported that CRISPR-Cas9 can be used to selectively target mutant HTT-associated SNPs, they also did not analyze whether gene editing could rescue motor deficits in an animal model of the disorder. Importantly, our results establish that CRISPR-Cas9-mediated disruption of the mutant HTT gene can significantly increase lifespan in R6/2 mice, which aggressively and rapidly manifest HD-like symptoms, and that gene editing can confer protection to neurons from striatal degeneration. Our results also demonstrate that CRISPR-Cas9 can provide a therapeutic benefit that is on par with those previously observed with an HTT-targeting ASO that was administered to the cerebrospinal fluid of R6/2 mice.¹⁸ Finally, compared to synthetic zinc-finger repressors, which were used to improve rotarod function and reduce clasping in R6/2 mice at 5 and 7 weeks of age,⁶⁷ we observed improved motor performance in mice from 10 to 14 weeks of age following Cas9-mediated gene editing.

Of note, past therapeutic gene-editing studies for HD have relied on the SpCas9 nuclease to facilitate modification of the HTT gene.^{59–61} Due to its relatively large size, the SpCas9 nuclease typically requires the use of two AAV particles for delivery with its sgRNA, a requirement that could reduce *in vivo* editing efficiency and limit therapeutic effectiveness. Our results show that SaCas9, a smaller Cas9 ortholog that can fit into a single AAV vector alongside an sgRNA and a

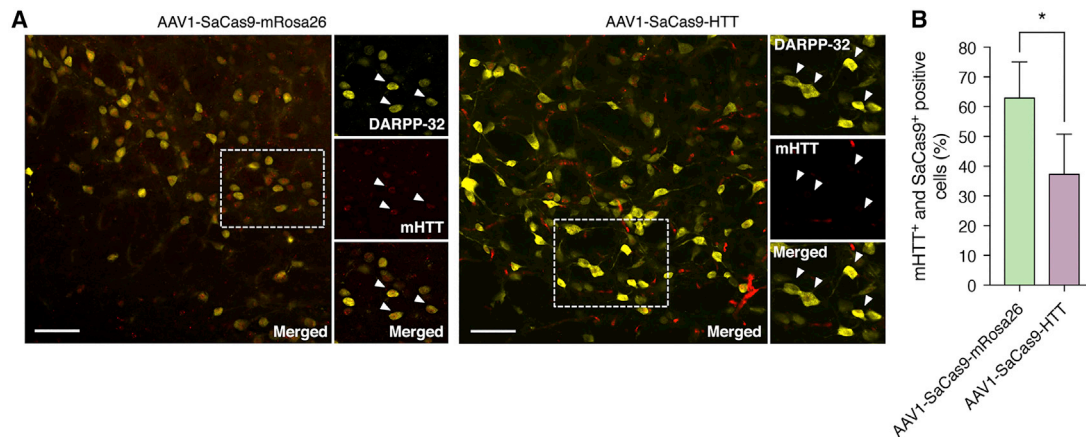


Figure 4. CRISPR-Cas9 Enhances Neuronal Survival in R6/2 Mice

(A) Immunofluorescent staining of end-stage striatal sections from R6/2 mice bilaterally injected with 6×10^{10} vector genomes of (left) AAV1-SaCas9-mRosa26 or (right) AAV1-SaCas9-HTT. Insets show high-magnification images. Arrowheads indicate representative DARPP-32⁺ and SaCas9⁺ cells with (left) high or (right) reduced mutant HTT (mHTT) protein. Images were captured using identical exposure conditions. Scale bars, 50 μ m. (B) Quantitation of immunohistochemical results from R6/2 mice injected with AAV1-SaCas9-HTT (n = 4) or AAV1-SaCas9-mRosa26 (n = 3). *p < 0.05, one-way unpaired t test.

promoter to drive its expression, can facilitate efficient disruption of the HTT gene, indicating that alternate CRISPR-Cas9 systems that are more accommodating to AAV-mediated delivery could be used to treat HD.

To effectively treat HD, CRISPR-Cas9 or any other gene-editing cargo must be efficiently delivered to the cell types affected by the disorder. Our immunohistochemical results indicated that ~85% of DARPP-32⁺ cells analyzed in the striatum expressed SaCas9 4 weeks after AAV delivery, indicating efficient transduction to the targeted area. However, other neuronal populations, including certain large pyramidal projection neurons,⁶⁸ are also vulnerable to HD-associated toxicity. Thus, directed evolution or other protein engineering strategies could be used to create specialized AAV capsid variants⁶⁹ that can facilitate enhanced delivery to all or most of the cell populations susceptible to HD. AAV vectors, in particular, hold tremendous potential as therapeutic gene delivery vehicles, as they have demonstrated efficacy in several clinical trials.^{70–74} In fact, a retina-directed AAV-based therapy earned regulatory approval by the U.S. Food and Drug Administration in 2017, the first such endorsement for an AAV therapy in the United States, with more potentially on the horizon. Additionally, while numerous advances have been made to help minimize the frequency that CRISPR-Cas9 nucleases introduce off-target mutations in cells,^{75–79} the continuous expression of Cas9 or any other gene-editing nuclease from an AAV vector could, nonetheless, cause off-target effects to accumulate. Self-inactivating gene-editing technologies^{61,80,81} such as the KamiCas9 system,⁶¹ which has been used to target the HTT gene in an HD mouse model, could be harnessed to limit the duration that a nuclease is exposed within a cell, though it remains to be seen whether such an approach can be integrated into an AAV vector. Further, to assess the safety of this therapeutic gene-editing strategy in a genetic background relevant to HD, unbiased methods for identifying Cas9-induced DSBs^{39,82,83} should

be performed in neurons differentiated from human induced pluripotent stem cells derived from HD patient cells in order to comprehensively curate sgRNA specificity. Though our analysis revealed no increase in indels at any analyzed candidate off-target cleavage site, the use of Cas9 variants with enhanced targeting specificity⁸⁴ could be used to help minimize the potential for off-target effects.

Finally, we note that, while treatment with CRISPR-Cas9 increased lifespan in R6/2 mice and protected some striatal neurons from death, the therapeutic genome-editing strategy described here is unable to restore lost cells. However, we⁸⁵ and others⁸⁶ have demonstrated that transplanted neural progenitors can innervate within a host tissue and form new synaptic connections with endogenous neurons.⁸⁵ Thus, in the future, CRISPR-Cas9-mediated gene editing could be used in combination with cell replacement therapy to treat HD via a two-step process that first involves CRISPR-mediated disruption of the endogenous mutant HTT gene to reduce its neurodegenerative effect and then involves the integration of a functional striatal graft to replace lost cells, thereby unifying the benefits of both approaches to treat HD in a potentially more effective manner.

In conclusion, we show that CRISPR-Cas9-mediated gene editing can reduce the formation of mutant HTT protein inclusions and provide therapeutic benefit to a mouse model of HD. Our results lay a foundation for using gene editing to treat HD and suggest that CRISPR-Cas9 and other emerging gene-editing technologies⁸⁷ have broad potential to treat neurodegenerative disorders.

MATERIALS AND METHODS

Plasmid Construction

The hSyn promoter was PCR amplified from pAAV-hSyn-mCherry (kindly provided by Dr. John Flannery) and cloned into the SpeI and AgeI sites of pAAV-CMV-SaCas9-U6-sgRNA (Addgene, #61591).

Exon 1 of the human HTT gene was searched for the motif 5'-(N)₂₀₋₂₁-NNGRRT-3' (where N = A, T, C, or G, and R = A or G) to identify potential SaCas9 cleavage sites. Oligonucleotides encoding the identified sgRNA targeting sequences were synthesized (Elim Biopharmaceuticals), phosphorylated by T4 polynucleotide kinase (New England Biolabs), annealed, and then ligated into the BsaI restriction sites of pAAV-hSyn-SaCas9-U6-sgRNA. Plasmid sequences were verified by DNA sequencing (UC Berkeley DNA Sequencing Facility) using the oligonucleotides described in [Table S1](#).

Cell Culture and Flow Cytometry

HEK293T cells were cultured in a 5% CO₂ atmosphere at 37°C and kept in DMEM (Corning) supplemented with 10% (v/v) fetal bovine serum (FBS; Life Technologies) and 1% (v/v) Antibiotic-Antimycotic (Anti-Anti; Life Technologies). For transfections, HEK293T cells were seeded onto 24-well plates at a density of 3×10^5 cells per well. At 16 h after seeding, cells were transfected with 100 ng pTreTight-HTT94Q-CFP (Addgene, #23966), 100 ng tTA/TRE-mCherry, and 800 ng pAAV-CMV-SaCas9-U6-sgRNA using 3 μ L polyethylenimine (1 μ g/ μ L), as described elsewhere.⁸⁸ At 72 h after transfection, cells were washed once with PBS, and mCherry and CFP fluorescence was evaluated by flow cytometry using a BD LSRFortessa X-20 cytometer (UC Berkeley Flow Cytometry Core Facility). For each sample, 50,000 live events were collected, and data were analyzed using FlowJo v10 (Tree Star)

Western Blot

Homogenized HEK293T cells transfected with 100 ng pTreTight-HTT94Q-CFP, 100 ng tTA/TRE-mCherry, and 800 ng pAAV-CMV-SaCas9-U6-sgRNA were lysed using RIPA buffer (50 mM Tris, 150 mM NaCl, 0.2% SDS, 0.5% deoxycholate, 1% NP-40, 1 mM EDTA [pH 8.0]) containing protease inhibitor cocktail (Sigma-Aldrich) for 30 min on ice and then centrifuged at $14,000 \times g$ for 5 min at 4°C. Supernatants were collected, and protein concentration was determined using the Pierce BCA Protein Assay Kit (Thermo Fisher Scientific) before 15 μ g protein was electrophoresed by SDS-PAGE and transferred onto a nitrocellulose membrane in transfer buffer (20 mM Tris-HCl, 150 mM glycine, and 20% [v/v] methanol) for 1 h at 160 V. Membranes were blocked with 5% (v/v) Blotting-Grade Blocker (Bio-Rad) in Tris-buffered saline (TBS) (20 mM Tris-HCl, 150 mM NaCl, [pH 7.5]) with 0.05% (v/v) Tween-20 (TBST) for 1 h and incubated overnight at 4°C with primary antibodies in blocking solution. The following antibodies were used: rabbit anti-GFP (Abcam, #ab6556) and rabbit anti-GAPDH, clone 14C10 (Cell Signaling, #2118). Membranes were washed three times with TBST and incubated with goat anti-rabbit secondary antibody horseradish peroxidase conjugate (Thermo Fisher Scientific, #65-6120) in blocking solution for 1 h at room temperature. After three washes with TBST, blots were developed using the SuperSignal West Dura Extended Duration Substrate (Thermo Fisher Scientific) and visualized by automated chemiluminescence using the Gel Doc XR Imaging System (Bio-Rad). Band intensity was quantitated using Image Lab (Bio-Rad). Total mutant HTT protein was normalized to GAPDH protein in each lane.

Harvested striatal tissue was lysed using RIPA buffer with 2% SDS, electrophoresed on a NuPAGE 4%–12% Bis-Tris Protein Gel (Thermo-Fisher Scientific), and transferred onto an Odyssey Nitrocellulose Membrane (Li-COR Biosciences). Membranes were incubated overnight at 4°C with the following primary antibodies: mouse anti-HTT, clone mEM48 (Millipore-Sigma, #MAB5374); and rabbit anti-GAPDH (Sigma-Aldrich). Membranes were washed three times with TBST and incubated with either biotinylated goat anti-rabbit immunoglobulin G (IgG) (Abcam, #ab64256) or biotinylated goat anti-mouse IgG (Abcam, #ab64255) in blocking solution for 1 h at room temperature. After three washes with TBST, blots were incubated with a streptavidin-Alexa Fluor 700 conjugate (Thermo Fisher Scientific, #S21383) for 1 h at room temperature and visualized using an Odyssey Imaging System. Band intensity was quantitated using Image Lab (Bio-Rad), and mutant HTT protein was normalized to GAPDH control protein in each lane.

Sanger Sequencing

HEK293T cells were seeded onto 24-well plates at a density of 3×10^5 cells per well and transfected with 100 ng tTA/TRE-mCherry and 800 ng pAAV-CMV-SaCas9-U6-sgRNA. At 72 h after transfection, mCherry⁺ cells were isolated using fluorescence-activated cell sorting (FACS) (BD FACSAria Fusion; UC Berkeley Flow Cytometry Core Facility), and genomic DNA was isolated using QuickExtract DNA Extraction Solution (Epicenter), according to the manufacturer's instructions. The mutant HTT transgene was PCR amplified using the primers EcoRI-HTT-Exon 1-Fwd and XbaI-HTT-Exon 1-Rev and cloned into the EcoRI and XbaI restriction sites in pcDNA 3.1(+). Individual colonies were mini-prepped and sequenced using the primers EcoRI-HTT-Exon 1-Fwd and XbaI-HTT-Exon 1-Rev.

AAV Vector Production

AAV was manufactured as described elsewhere.⁸⁸ Briefly, HEK293T cells were seeded onto 15-cm plates at a density of 4×10^7 cells per plate in DMEM with 10% (v/v) FBS and 1% Anti-Anti. At 16 h after seeding, cells were transfected with 15 μ g pHelper, 15 μ g AAV1, and 15 μ g either pAAV-hSyn-SaCas9-U6-sgRNA-HTT or pAAV-hSyn-SaCas9-U6-sgRNA-mRosa25 using 135 μ L polyethylamine (1 μ g/ μ L). At 48 h after transfection, cells were harvested and centrifuged at $4,000 \times g$ for 5 min at room temperature and freeze-thawed three times in lysis buffer (50 mM Tris-HCl, 150 mM NaCl [pH 8.0]). Cell lysate was incubated with 10 U benzonase nuclease (Sigma-Aldrich) for 30 min at 37°C and centrifuged at $10,000 \times g$ for 10 min at room temperature. Supernatant was collected and laid over an iodixanol gradient and centrifuged at $42,000 \times g$ for 2 h at 18°C. AAV was extracted from the iodixanol gradient and buffer exchanged with PBS with 0.001% Tween-20 using an Ultra-15 Centrifugal Filter Unit (Amicon) at $4,000 \times g$ and concentrated to $\sim 200 \mu$ L. Virus was stored at 4°C, and the genomic titer was determined by qRT-PCR using SYBR Green (Sigma-Aldrich), as described elsewhere.⁸⁸

Injections

Animal procedures were approved by the Office of Laboratory Animal Care at UC Berkeley and conducted in accordance with the

NIH Guide for the Care and Use of Laboratory Animals. Four-week-old R6/2 mice bred from 8-week-old R6/2 mice (B6CBA-Tg(HDexon1)62Gpb/3J; Jackson Laboratory, stock #006494) and 8-week-old female B6CBAF1 mice (Jackson Laboratory, stock #100011) were bilaterally injected with 2×10^{10} vector genomes of AAV1-hSyn-SaCas9-HTT or AAV1-hSyn-SaCas9-mRosa26 in 2 μ L PBS with 0.001% Tween-20 at stereotaxic coordinates anterior-posterior (AP) = 0.50 mm; medial-lateral (ML) = ± 1.75 mm; and dorsal-ventral (DV) = -2.0 mm, -1.5 mm, and -1 mm using a 10- μ L syringe with a 22G Point Style 4 needle with a 30° angle (Hamilton). Before injections, animals were genotyped by PCR using genomic DNA purified from an ear clip.

Behavior

Starting 2 weeks after injections, treated and control R6/2 mice were monitored weekly with the rotarod assay, clasping test, and weight measurements. Treatment groups were gender balanced, and all measurements were performed in a blinded manner. For the rotarod, mice were placed onto a Rotamex-5 rotarod (Columbus Instruments), and the latency to fall (measured in seconds) was recorded for each animal. Each session consisted of three trials, with the rotarod programmed to accelerate from 4 to 40 rpm in 180 s. For the clasping test, mice were suspended by the tail for 30 s and scored from 0 to 3: 0 = no clasping was observed; 1 = mice clasped hindlimbs within 30 s; 2 = mice clasped hindlimbs but recovered within 5 s when released; and 3 = mice clasped hindlimbs but failed to recover within 5 s when released. All data were normalized to values determined at week 8 (i.e., 4 weeks after injection). End-stage was defined as the point at which animals were moribund, lacked a righting reflex, failed to respond to gentle stimulation, or decreased to 80% of their peak weight.

Striatal Tissue Harvesting

Mice were anesthetized by intraperitoneal injection of ketamine (100 mg/kg) and xylazine (10 mg/kg) and transcardially perfused with 0.9% saline. Brains were harvested, and the striatum was isolated by manual dissection on a pre-chilled surface. Tissue was homogenized by incubation in trypsin for 90 min at 37°C with constant CO₂ equilibration and gentle perturbation every 15 min. Cells were centrifuged at $2,000 \times g$ for 5 min at room temperature, washed once with PBS, and then centrifuged for an additional $2,000 \times g$ for 5 min at room temperature.

Deep Sequencing

Candidate OT sites were identified using Cas-OFFinder, as described elsewhere.⁴⁶ Briefly, the mm10 mouse reference genome was searched for sites with, at most, four mismatches (up to two nucleotide mismatches and up to two DNA or sgRNA bulges) from the sgRNA target site in the human HTT gene. The 10 most similar sites were chosen for analysis. Striatal tissue from R6/2 mice injected with AAV1-SaCas9-HTT or AAV1-SaCas9-mRosa26 was harvested, and genomic DNA was extracted using the DNeasy Blood & Tissue Kit (QIAGEN). The sgRNA target site in the human HTT gene and the candidate off-target cleavage site in the mouse HTT gene were

amplified (Table S1) using a touchdown PCR with Taq DNA Polymerase (New England Biolabs). The remaining candidate off-target sites were amplified (Table S1) using Phusion High-Fidelity DNA Polymerase (New England Biolabs). Mouse-specific barcode sequences were then incorporated using an additional round of PCR. All barcoded amplicons were quantified using PicoGreen (Thermo Fisher Scientific) and purified using AMPure PCR purification (Beckman) at the UC Berkeley Functional Genomics Laboratory. Barcoded amplicons were pooled together, and 150-bp single-ended reads were generated using the HiSeq 4000 System (Illumina; QB3 Vincent J. Coates Genomics Sequencing Laboratory). Samples were demultiplexed based on their index, and adaptor sequences were trimmed from the reads. Using CRISPResso, sequences were filtered for >99% confidence (phred33 threshold > 20) and aligned using EMBOSS Needle. Indel frequency was quantified within a 25-bp window of the cleavage site (substitutions were ignored). Samples with fewer than 1,000 reads post-analysis were removed from statistical analysis.

Immunofluorescence Staining

Mice were anesthetized by intraperitoneal injection of ketamine (100 mg/kg) and xylazine (10 mg/kg) and transcardially perfused with 0.9% saline followed by 4% paraformaldehyde. Brains were harvested and post-fixed in 4% paraformaldehyde for 48 h at 4°C and then transferred to a 30% (w/v) sucrose solution. Brains were cut to 40- μ m coronal sections and stored in cytoprotectant at -20°C . Sections were then washed three times with PBS, incubated with blocking solution (PBS with 2% [v/v] BSA, 5% [v/v] donkey serum, and 0.2% [v/v] Triton X-100) at room temperature for 2 h, and stained with primary antibodies in blocking solution for 48 h at 4°C. Sections were washed four times with PBS and incubated with secondary antibodies in blocking solution for 2 h followed by a 10-min incubation with DAPI nuclear stain. After staining, sections were washed four times with PBS, mounted onto slides, and visualized using a Zeiss LSM 710 AxioObserver confocal microscope (UC Berkeley Molecular Imaging Center). Image analysis was performed using ImageJ (<https://imagej.nih.gov/ij/>).

The following antibodies were used for brain sections: mouse anti-HTT, clone mEM48 (Millipore-Sigma, #MAB5374); goat anti-DARPP-32 (R&D Systems, #AF6259); and rabbit anti-HA, clone C29F4 (Cell Signaling Technology, #3724). The following secondary antibodies were used: donkey anti-goat Alexa Fluor 488 (Jackson ImmunoResearch Laboratories, #703-545-155), donkey anti-rabbit Alexa Fluor 555 (Thermo-Fisher Scientific, #A-31572), and donkey anti-mouse Alexa Fluor 647 (Thermo-Fisher Scientific, #A-31571).

Statistics

Statistical analysis was performed using Prism 7 (GraphPad Software). Mutant HTT protein, mean lifespan, and neuron survival were compared using an unpaired t test. Rotarod times, weight loss, and clasping scores were compared using a one-way ANOVA followed by Tukey's post hoc analysis. Kaplan-Meier plots were analyzed using the log-rank test.

SUPPLEMENTAL INFORMATION

Supplemental Information can be found online at <https://doi.org/10.1016/j.omtn.2019.07.009>.

AUTHOR CONTRIBUTIONS

T.G. and D.V.S. conceived of the study. F.K.E. designed constructs; performed molecular biology; packaged the AAV vector; performed injections, behavior studies, and immunofluorescent staining; and analyzed the data. D.S.O. performed molecular biology and animal studies. M.M.A. performed injections and immunofluorescent staining. P.A.L. performed next-generation sequencing and western blot. T.G. designed the experiments, performed molecular biology studies, and analyzed the data. T.G. and F.K.E. wrote the manuscript, with contributions from all authors.

CONFLICTS OF INTEREST

D.V.S. is an inventor on patents related to AAV vectors and cofounder of 4D Molecular Therapeutics, a company focused on the clinical development of gene therapies for recessive diseases using engineered AAV variants. D.V.S. is also a member of the board of directors of uniQure, a company focused on clinical AAV gene therapy. D.S.O. is now an employee of Sangamo Therapeutics. T.G. is a consultant for 4D Molecular Therapeutics. F.K.E., M.M.A., and P.A.L. declare no competing interests.

ACKNOWLEDGMENTS

We thank J.G. Flannery for providing space for behavioral studies, A. Dillin for providing the rotarod, S. Kumar for access to the Odyssey Imaging system, and G.N. Ramadoss for technical assistance. T.G. was supported by a Ruth L. Kirschstein National Research Service Award (NRSA) (F32GM113446) and by the Judith and Jean Pape Adams Charitable Foundation. D.S.O. was supported by an NSF Graduate Research Fellowship and a UC Berkeley Dissertation-Year Fellowship. D.V.S. was supported by the NIH (R01EY022975) and a gift from D. Chan.

REFERENCES

- Bates, G.P., Dorsey, R., Gusella, J.F., Hayden, M.R., Kay, C., Leavitt, B.R., Nance, M., Ross, C.A., Scahill, R.I., Wetzel, R., et al. (2015). Huntington disease. *Nat. Rev. Dis. Primers* *1*, 15005.
- MacDonald, M.E., Ambrose, C.M., Duyao, M.P., Myers, R.H., Lin, C., Srinidhi, L., Barnes, G., Taylor, S.A., James, M., Groot, N., et al. (1993). A novel gene containing a trinucleotide repeat that is expanded and unstable on Huntington's disease chromosomes. *Cell* *72*, 971–983.
- Gutkunst, C.A., Li, S.H., Yi, H., Mulroy, J.S., Kuemmerle, S., Jones, R., Rye, D., Ferrante, R.J., Hersch, S.M., and Li, X.J. (1999). Nuclear and neuropil aggregates in Huntington's disease: relationship to neuropathology. *J. Neurosci.* *19*, 2522–2534.
- Kim, Y.J., Yi, Y., Sapp, E., Wang, Y., Cuiffo, B., Kegel, K.B., Qin, Z.H., Aronin, N., and DiFiglia, M. (2001). Caspase 3-cleaved N-terminal fragments of wild-type and mutant huntingtin are present in normal and Huntington's disease brains, associate with membranes, and undergo calpain-dependent proteolysis. *Proc. Natl. Acad. Sci. USA* *98*, 12784–12789.
- Grima, J.C., Daigle, J.G., Arbez, N., Cunningham, K.C., Zhang, K., Ochaba, J., Geater, C., Morozko, E., Stocksdale, J., Glatzer, J.C., et al. (2017). Mutant huntingtin disrupts the nuclear pore complex. *Neuron* *94*, 93–107.e6.
- DiFiglia, M., Sapp, E., Chase, K.O., Davies, S.W., Bates, G.P., Vonsattel, J.P., and Aronin, N. (1997). Aggregation of huntingtin in neuronal intranuclear inclusions and dystrophic neurites in brain. *Science* *277*, 1990–1993.
- Scherzinger, E., Lurz, R., Turmaine, M., Mangiarini, L., Hollenbach, B., Hasenbank, R., Bates, G.P., Davies, S.W., Lehrach, H., and Wanker, E.E. (1997). Huntingtin-encoded polyglutamine expansions form amyloid-like protein aggregates in vitro and in vivo. *Cell* *90*, 549–558.
- Waldvogel, H.J., Kim, E.H., Tippett, L.J., Vonsattel, J.P., and Faull, R.L. (2015). The neuropathology of Huntington's disease. *Curr. Top. Behav. Neurosci.* *22*, 33–80.
- Vonsattel, J.P., Myers, R.H., Stevens, T.J., Ferrante, R.J., Bird, E.D., and Richardson, E.P., Jr. (1985). Neuropathological classification of Huntington's disease. *J. Neuropathol. Exp. Neurol.* *44*, 559–577.
- Ross, C.A., Aylward, E.H., Wild, E.J., Langbehn, D.R., Long, J.D., Warner, J.H., Scahill, R.I., Leavitt, B.R., Stout, J.C., Paulsen, J.S., et al. (2014). Huntington disease: natural history, biomarkers and prospects for therapeutics. *Nat. Rev. Neurol.* *10*, 204–216.
- Yamamoto, A., Lucas, J.J., and Hen, R. (2000). Reversal of neuropathology and motor dysfunction in a conditional model of Huntington's disease. *Cell* *101*, 57–66.
- Díaz-Hernández, M., Torres-Peraza, J., Salvatori-Abarca, A., Morán, M.A., Gómez-Ramos, P., Alberch, J., and Lucas, J.J. (2005). Full motor recovery despite striatal neuron loss and formation of irreversible amyloid-like inclusions in a conditional mouse model of Huntington's disease. *J. Neurosci.* *25*, 9773–9781.
- Harper, S.Q., Staber, P.D., He, X., Eliason, S.L., Martins, I.H., Mao, Q., Yang, L., Kotin, R.M., Paulson, H.L., and Davidson, B.L. (2005). RNA interference improves motor and neuropathological abnormalities in a Huntington's disease mouse model. *Proc. Natl. Acad. Sci. USA* *102*, 5820–5825.
- Boudreau, R.L., McBride, J.L., Martins, I., Shen, S., Xing, Y., Carter, B.J., and Davidson, B.L. (2009). Nonallele-specific silencing of mutant and wild-type huntingtin demonstrates therapeutic efficacy in Huntington's disease mice. *Mol. Ther.* *17*, 1053–1063.
- Drouet, V., Perrin, V., Hassig, R., Dufour, N., Auregan, G., Alves, S., Bonvento, G., Brouillet, E., Luthi-Carter, R., Hantraye, P., and Déglon, N. (2009). Sustained effects of nonallele-specific huntingtin silencing. *Ann. Neurol.* *65*, 276–285.
- Carroll, J.B., Warby, S.C., Southwell, A.L., Doty, C.N., Greenlee, S., Skotte, N., Hung, G., Bennett, C.F., Freier, S.M., and Hayden, M.R. (2011). Potent and selective antisense oligonucleotides targeting single-nucleotide polymorphisms in the Huntington disease gene / allele-specific silencing of mutant huntingtin. *Mol. Ther.* *19*, 2178–2185.
- Southwell, A.L., Skotte, N.H., Bennett, C.F., and Hayden, M.R. (2012). Antisense oligonucleotide therapeutics for inherited neurodegenerative diseases. *Trends Mol. Med.* *18*, 634–643.
- Kordasiewicz, H.B., Stanek, L.M., Wancewicz, E.V., Mazur, C., McAlonis, M.M., Pytel, K.A., Artates, J.W., Weiss, A., Cheng, S.H., Shihabuddin, L.S., et al. (2012). Sustained therapeutic reversal of Huntington's disease by transient repression of huntingtin synthesis. *Neuron* *74*, 1031–1044.
- Drouet, V., Ruiz, M., Zala, D., Feyeux, M., Auregan, G., Cambon, K., Troquier, L., Carpentier, J., Aubert, S., Merienne, N., et al. (2014). Allele-specific silencing of mutant huntingtin in rodent brain and human stem cells. *PLoS ONE* *9*, e99341.
- Miniarikova, J., Zimmer, V., Martier, R., Brouwers, C.C., Pythoud, C., Richetin, K., Rey, M., Lubelski, J., Evers, M.M., van Deventer, S.J., et al. (2017). AAV5-miHTT gene therapy demonstrates suppression of mutant huntingtin aggregation and neuronal dysfunction in a rat model of Huntington's disease. *Gene Ther.* *24*, 630–639.
- Evers, M.M., Miniarikova, J., Juhas, S., Vallès, A., Bohuslavova, B., Juhasova, J., Skalnikova, H.K., Vodicka, P., Valekova, I., Brouwers, C., et al. (2018). AAV5-miHTT gene therapy demonstrates broad distribution and strong human mutant huntingtin lowering in a Huntington's disease minipig model. *Mol. Ther.* *26*, 2163–2177.
- Miniarikova, J., Zanella, I., Huseinovic, A., van der Zon, T., Hanemaaijer, E., Martier, R., Koornneef, A., Southwell, A.L., Hayden, M.R., van Deventer, S.J., et al. (2016). Design, characterization, and lead selection of therapeutic miRNAs targeting huntingtin for development of gene therapy for huntington's disease. *Mol. Ther. Nucleic Acids* *5*, e297.

23. Jackson, A.L., Bartz, S.R., Schelter, J., Kobayashi, S.V., Burchard, J., Mao, M., Li, B., Cavet, G., and Linsley, P.S. (2003). Expression profiling reveals off-target gene regulation by RNAi. *Nat. Biotechnol.* 21, 635–637.
24. Jackson, A.L., Burchard, J., Schelter, J., Chau, B.N., Cleary, M., Lim, L., and Linsley, P.S. (2006). Widespread siRNA “off-target” transcript silencing mediated by seed region sequence complementarity. *RNA* 12, 1179–1187.
25. Singh, S., Narang, A.S., and Mahato, R.I. (2011). Subcellular fate and off-target effects of siRNA, shRNA, and miRNA. *Pharm. Res.* 28, 2996–3015.
26. Gaj, T., Sirk, S.J., Shui, S.L., and Liu, J. (2016). Genome-editing technologies: principles and applications. *Cold Spring Harb. Perspect. Biol.* 8, a023754.
27. Jinek, M., Chylinski, K., Fonfara, I., Hauer, M., Doudna, J.A., and Charpentier, E. (2012). A programmable dual-RNA-guided DNA endonuclease in adaptive bacterial immunity. *Science* 337, 816–821.
28. Cong, L., Ran, F.A., Cox, D., Lin, S., Barretto, R., Habib, N., Hsu, P.D., Wu, X., Jiang, W., Marraffini, L.A., and Zhang, F. (2013). Multiplex genome engineering using CRISPR/Cas systems. *Science* 339, 819–823.
29. Mali, P., Yang, L., Esvelt, K.M., Aach, J., Guell, M., DiCarlo, J.E., Norville, J.E., and Church, G.M. (2013). RNA-guided human genome engineering via Cas9. *Science* 339, 823–826.
30. Jinek, M., East, A., Cheng, A., Lin, S., Ma, E., and Doudna, J. (2013). RNA-programmed genome editing in human cells. *eLife* 2, e00471.
31. Cho, S.W., Kim, S., Kim, J.M., and Kim, J.S. (2013). Targeted genome engineering in human cells with the Cas9 RNA-guided endonuclease. *Nat. Biotechnol.* 31, 230–232.
32. Maeder, M.L., and Gersbach, C.A. (2016). Genome-editing technologies for gene and cell therapy. *Mol. Ther.* 24, 430–446.
33. Santiago, Y., Chan, E., Liu, P.Q., Orlando, S., Zhang, L., Urnov, F.D., Holmes, M.C., Guschin, D., Waite, A., Miller, J.C., et al. (2008). Targeted gene knockout in mammalian cells by using engineered zinc-finger nucleases. *Proc. Natl. Acad. Sci. USA* 105, 5809–5814.
34. Hentze, M.W., and Kulozik, A.E. (1999). A perfect message: RNA surveillance and nonsense-mediated decay. *Cell* 96, 307–310.
35. Ojala, D.S., Amara, D.P., and Schaffer, D.V. (2015). Adeno-associated virus vectors and neurological gene therapy. *Neuroscientist* 21, 84–98.
36. Lentz, T.B., Gray, S.J., and Samulski, R.J. (2012). Viral vectors for gene delivery to the central nervous system. *Neurobiol. Dis.* 48, 179–188.
37. Aschauer, D.F., Kreuz, S., and Rumpel, S. (2013). Analysis of transduction efficiency, tropism and axonal transport of AAV serotypes 1, 2, 5, 6, 8 and 9 in the mouse brain. *PLoS ONE* 8, e76310.
38. Gaj, T., Epstein, B.E., and Schaffer, D.V. (2016). Genome engineering using adeno-associated virus: basic and clinical research applications. *Mol. Ther.* 24, 458–464.
39. Ran, F.A., Cong, L., Yan, W.X., Scott, D.A., Gootenberg, J.S., Kriz, A.J., Zetsche, B., Shalem, O., Wu, X., Makarova, K.S., et al. (2015). *In vivo* genome editing using *Staphylococcus aureus* Cas9. *Nature* 520, 186–191.
40. Maynard, C.J., Böttcher, C., Ortega, Z., Smith, R., Florea, B.I., Díaz-Hernández, M., Brundin, P., Overkleeft, H.S., Li, J.Y., Lucas, J.J., and Dantuma, N.P. (2009). Accumulation of ubiquitin conjugates in a polyglutamine disease model occurs without global ubiquitin/proteasome system impairment. *Proc. Natl. Acad. Sci. USA* 106, 13986–13991.
41. Mangiarini, L., Sathasivam, K., Seller, M., Cozens, B., Harper, A., Hetherington, C., Lawton, M., Trotter, Y., Leach, H., Davies, S.W., and Bates, G.P. (1996). Exon 1 of the HD gene with an expanded CAG repeat is sufficient to cause a progressive neurological phenotype in transgenic mice. *Cell* 87, 493–506.
42. Chiang, C., Jacobsen, J.C., Ernst, C., Hanscom, C., Heilbut, A., Blumenthal, I., Mills, R.E., Kirby, A., Lindgren, A.M., Rudiger, S.R., et al. (2012). Complex reorganization and predominant non-homologous repair following chromosomal breakage in karyotypically balanced germline rearrangements and transgenic integration. *Nat. Genet.* 44, 390–397.
43. Menalled, L., El-Khodori, B.F., Patry, M., Suárez-Fariñas, M., Orenstein, S.J., Zahasky, B., Leahy, C., Wheeler, V., Yang, X.W., MacDonald, M., et al. (2009). Systematic behavioral evaluation of Huntington’s disease transgenic and knock-in mouse models. *Neurobiol. Dis.* 35, 319–336.
44. Cummings, D.M., Alaghband, Y., Hickey, M.A., Joshi, P.R., Hong, S.C., Zhu, C., Ando, T.K., André, V.M., Cepeda, C., Watson, J.B., and Levine, M.S. (2012). A critical window of CAG repeat-length correlates with phenotype severity in the R6/2 mouse model of Huntington’s disease. *J. Neurophysiol.* 107, 677–691.
45. Irion, S., Luche, H., Gadue, P., Fehling, H.J., Kennedy, M., and Keller, G. (2007). Identification and targeting of the ROSA26 locus in human embryonic stem cells. *Nat. Biotechnol.* 25, 1477–1482.
46. Gaj, T., Ojala, D.S., Ekman, F.K., Byrne, L.C., Limsirichai, P., and Schaffer, D.V. (2017). *In vivo* genome editing improves motor function and extends survival in a mouse model of ALS. *Sci. Adv.* 3, eaar3952.
47. Hadaczek, P., Stanek, L., Ciesielska, A., Sudhakar, V., Samaranch, L., Pivrotto, P., Bringas, J., O’Riordan, C., Mastis, B., San Sebastian, W., et al. (2016). Widespread AAV1- and AAV2-mediated transgene expression in the nonhuman primate brain: implications for Huntington’s disease. *Mol. Ther. Methods Clin. Dev.* 3, 16037.
48. Connor, B., Sun, Y., von Hieber, D., Tang, S.K., Jones, K.S., and Maucksch, C. (2016). AAV1/2-mediated BDNF gene therapy in a transgenic rat model of Huntington’s disease. *Gene Ther.* 23, 283–295.
49. Franich, N.R., Fitzsimons, H.L., Fong, D.M., Klugmann, M., Doring, M.J., and Young, D. (2008). AAV vector-mediated RNAi of mutant huntingtin expression is neuroprotective in a novel genetic rat model of Huntington’s disease. *Mol. Ther.* 16, 947–956.
50. Wang, C.E., Zhou, H., McGuire, J.R., Cerullo, V., Lee, B., Li, S.H., and Li, X.J. (2008). Suppression of neuropil aggregates and neurological symptoms by an intracellular antibody implicates the cytoplasmic toxicity of mutant huntingtin. *J. Cell Biol.* 181, 803–816.
51. Pinello, L., Canver, M.C., Hoban, M.D., Orkin, S.H., Kohn, D.B., Bauer, D.E., and Yuan, G.C. (2016). Analyzing CRISPR genome-editing experiments with CRISPResso. *Nat. Biotechnol.* 34, 695–697.
52. Bae, S., Park, J., and Kim, J.S. (2014). Cas-OFFinder: a fast and versatile algorithm that searches for potential off-target sites of Cas9 RNA-guided endonucleases. *Bioinformatics* 30, 1473–1475.
53. Morton, A.J., Lagan, M.A., Skepper, J.N., and Dunnett, S.B. (2000). Progressive formation of inclusions in the striatum and hippocampus of mice transgenic for the human Huntington’s disease mutation. *J. Neurocytol.* 29, 679–702.
54. Meade, C.A., Deng, Y.P., Fusco, F.R., Del Mar, N., Hersch, S., Goldowitz, D., and Reiner, A. (2002). Cellular localization and development of neuronal intranuclear inclusions in striatal and cortical neurons in R6/2 transgenic mice. *J. Comp. Neurol.* 449, 241–269.
55. Ehrnhoefer, D.E., Butland, S.L., Pouladi, M.A., and Hayden, M.R. (2009). Mouse models of Huntington disease: variations on a theme. *Dis. Model. Mech.* 2, 123–129.
56. Rawlins, M.D., Wexler, N.S., Wexler, A.R., Tabrizi, S.J., Douglas, I., Evans, S.J., and Smeeth, L. (2016). The prevalence of Huntington’s disease. *Neuroepidemiology* 46, 144–153.
57. Tervo, D.G., Hwang, B.Y., Viswanathan, S., Gaj, T., Lavzin, M., Ritola, K.D., Lindo, S., Michael, S., Kuleshova, E., Ojala, D., et al. (2016). A designer AAV variant permits efficient retrograde access to projection neurons. *Neuron* 92, 372–382.
58. Swiech, L., Heidenreich, M., Banerjee, A., Habib, N., Li, Y., Trombetta, J., Sur, M., and Zhang, F. (2015). *In vivo* interrogation of gene function in the mammalian brain using CRISPR-Cas9. *Nat. Biotechnol.* 33, 102–106.
59. Yang, S., Chang, R., Yang, H., Zhao, T., Hong, Y., Kong, H.E., Sun, X., Qin, Z., Jin, P., Li, S., and Li, X.J. (2017). CRISPR/Cas9-mediated gene editing ameliorates neurotoxicity in mouse model of Huntington’s disease. *J. Clin. Invest.* 127, 2719–2724.
60. Monteys, A.M., Ebanks, S.A., Keiser, M.S., and Davidson, B.L. (2017). CRISPR/Cas9 editing of the mutant huntingtin allele *in vitro* and *in vivo*. *Mol. Ther.* 25, 12–23.
61. Merienne, N., Vachey, G., de Longprez, L., Meunier, C., Zimmer, V., Perriard, G., Canales, M., Mathias, A., Herrgott, L., Beltraminelli, T., et al. (2017). The self-inactivating KamiCas9 system for the editing of CNS disease genes. *Cell Rep.* 20, 2980–2991.
62. Suzuki, K., Tsunekawa, Y., Hernandez-Benitez, R., Wu, J., Zhu, J., Kim, E.J., Hatanaka, F., Yamamoto, M., Araoka, T., Li, Z., et al. (2016). *In vivo* genome editing via CRISPR/Cas9 mediated homology-independent targeted integration. *Nature* 540, 144–149.

63. Ferrante, R.J. (2009). Mouse models of Huntington's disease and methodological considerations for therapeutic trials. *Biochim. Biophys. Acta* 1792, 506–520.
64. Nasir, J., Floresco, S.B., O'Kusky, J.R., Diewert, V.M., Richman, J.M., Zeisler, J., Borowski, A., Marth, J.D., Phillips, A.G., and Hayden, M.R. (1995). Targeted disruption of the Huntington's disease gene results in embryonic lethality and behavioral and morphological changes in heterozygotes. *Cell* 81, 811–823.
65. Duyao, M.P., Auerbach, A.B., Ryan, A., Persichetti, F., Barnes, G.T., McNeil, S.M., Ge, P., Vonsattel, J.P., Gusella, J.F., Joyner, A.L., et al. (1995). Inactivation of the mouse Huntington's disease gene homolog Hdh. *Science* 269, 407–410.
66. Wang, G., Liu, X., Gaertig, M.A., Li, S., and Li, X.J. (2016). Ablation of huntingtin in adult neurons is nondeleterious but its depletion in young mice causes acute pancreatitis. *Proc. Natl. Acad. Sci. USA* 113, 3359–3364.
67. Garriga-Canut, M., Agustín-Pavón, C., Herrmann, F., Sánchez, A., Dierssen, M., Fillat, C., and Isalan, M. (2012). Synthetic zinc finger repressors reduce mutant huntingtin expression in the brain of R6/2 mice. *Proc. Natl. Acad. Sci. USA* 109, E3136–E3145.
68. Han, I., You, Y., Kordower, J.H., Brady, S.T., and Morfini, G.A. (2010). Differential vulnerability of neurons in Huntington's disease: the role of cell type-specific features. *J. Neurochem.* 113, 1073–1091.
69. Kotterman, M.A., and Schaffer, D.V. (2014). Engineering adeno-associated viruses for clinical gene therapy. *Nat. Rev. Genet.* 15, 445–451.
70. Nathwani, A.C., Reiss, U.M., Tuddenham, E.G., Rosales, C., Chowdhury, P., McIntosh, J., Della Peruta, M., Lheriteau, E., Patel, N., Raj, D., et al. (2014). Long-term safety and efficacy of factor IX gene therapy in hemophilia B. *N. Engl. J. Med.* 371, 1994–2004.
71. MacLaren, R.E., Groppe, M., Barnard, A.R., Cottrill, C.L., Tolmachova, T., Seymour, L., Clark, K.R., During, M.J., Cremers, F.P., Black, G.C., et al. (2014). Retinal gene therapy in patients with choroideremia: initial findings from a phase 1/2 clinical trial. *Lancet* 383, 1129–1137.
72. Stroes, E.S., Nierman, M.C., Meulenberg, J.J., Franssen, R., Twisk, J., Henny, C.P., Maas, M.M., Zwinderman, A.H., Ross, C., Aronica, E., et al. (2008). Intramuscular administration of AAV1-lipoprotein lipase S447X lowers triglycerides in lipoprotein lipase-deficient patients. *Arterioscler. Thromb. Vasc. Biol.* 28, 2303–2304.
73. Carpentier, A.C., Frisch, F., Labbé, S.M., Gagnon, R., de Wal, J., Greentree, S., Petry, H., Twisk, J., Brisson, D., and Gaudet, D. (2012). Effect of alipogene tiparovec (AAV1-LPL(S447X)) on postprandial chylomicron metabolism in lipoprotein lipase-deficient patients. *J. Clin. Endocrinol. Metab.* 97, 1635–1644.
74. Bainbridge, J.W., Smith, A.J., Barker, S.S., Robbie, S., Henderson, R., Balaggan, K., Viswanathan, A., Holder, G.E., Stockman, A., Tyler, N., et al. (2008). Effect of gene therapy on visual function in Leber's congenital amaurosis. *N. Engl. J. Med.* 358, 2231–2239.
75. Hsu, P.D., Scott, D.A., Weinstein, J.A., Ran, F.A., Konermann, S., Agarwala, V., Li, Y., Fine, E.J., Wu, X., Shalem, O., et al. (2013). DNA targeting specificity of RNA-guided Cas9 nucleases. *Nat. Biotechnol.* 31, 827–832.
76. Doench, J.G., Hartenian, E., Graham, D.B., Tothova, Z., Hegde, M., Smith, I., Sullender, M., Ebert, B.L., Xavier, R.J., and Root, D.E. (2014). Rational design of highly active sgRNAs for CRISPR-Cas9-mediated gene inactivation. *Nat. Biotechnol.* 32, 1262–1267.
77. Fu, Y., Sander, J.D., Reyon, D., Cascio, V.M., and Joung, J.K. (2014). Improving CRISPR-Cas nuclease specificity using truncated guide RNAs. *Nat. Biotechnol.* 32, 279–284.
78. Guilinger, J.P., Thompson, D.B., and Liu, D.R. (2014). Fusion of catalytically inactive Cas9 to FokI nuclease improves the specificity of genome modification. *Nat. Biotechnol.* 32, 577–582.
79. Tsai, S.Q., Wyvekens, N., Khayter, C., Foden, J.A., Thapar, V., Reyon, D., Goodwin, M.J., Aryee, M.J., and Joung, J.K. (2014). Dimeric CRISPR RNA-guided FokI nucleases for highly specific genome editing. *Nat. Biotechnol.* 32, 569–576.
80. Chen, Y., Liu, X., Zhang, Y., Wang, H., Ying, H., Liu, M., Li, D., Lui, K.O., and Ding, Q. (2016). A self-restricted CRISPR system to reduce off-target effects. *Mol. Ther.* 24, 1508–1510.
81. Petris, G., Casini, A., Montagna, C., Lorenzin, F., Prandi, D., Romanel, A., Zasso, J., Conti, L., Demichelis, F., and Cereseto, A. (2017). Hit and go CAS9 delivered through a lentiviral based self-limiting circuit. *Nat. Commun.* 8, 15334.
82. Tsai, S.Q., Zheng, Z., Nguyen, N.T., Liebers, M., Topkar, V.V., Thapar, V., Wyvekens, N., Khayter, C., Iafate, A.J., Le, L.P., et al. (2015). GUIDE-seq enables genome-wide profiling of off-target cleavage by CRISPR-Cas nucleases. *Nat. Biotechnol.* 33, 187–197.
83. Kim, D., Bae, S., Park, J., Kim, E., Kim, S., Yu, H.R., Hwang, J., Kim, J.I., and Kim, J.S. (2015). Digenome-seq: genome-wide profiling of CRISPR-Cas9 off-target effects in human cells. *Nat. Methods* 12, 237–243, 1, 243.
84. Slaymaker, I.M., Gao, L., Zetsche, B., Scott, D.A., Yan, W.X., and Zhang, F. (2016). Rationally engineered Cas9 nucleases with improved specificity. *Science* 351, 84–88.
85. Adil, M.M., Gaj, T., Rao, A.T., Kulkarni, R.U., Fuentes, C.M., Ramadoss, G.N., Ekman, F.K., Miller, E.W., and Schaffer, D.V. (2018). hPSC-derived striatal cells generated using a scalable 3D hydrogel promote recovery in a Huntington disease mouse model. *Stem Cell Reports* 10, 1481–1491.
86. Reidling, J.C., Relaño-Ginés, A., Holley, S.M., Ochaba, J., Moore, C., Fury, B., Lau, A., Tran, A.H., Yeung, S., Salamati, D., et al. (2018). Human neural stem cell transplantation rescues functional deficits in R6/2 and Q140 Huntington's disease mice. *Stem Cell Reports* 10, 58–72.
87. Brooks, A.K., and Gaj, T. (2018). Innovations in CRISPR technology. *Curr. Opin. Biotechnol.* 52, 95–101.
88. Gaj, T., and Schaffer, D.V. (2016). Adeno-associated virus-mediated delivery of CRISPR-Cas systems for genome engineering in mammalian cells. *Cold Spring Harb. Protoc.* 2016, <https://doi.org/10.1101/pdb.prot086868>.

OMTN, Volume 17

Supplemental Information

CRISPR-Cas9-Mediated Genome Editing Increases Lifespan and Improves Motor Deficits in a Huntington's Disease Mouse Model

Freja K. Ekman, David S. Ojala, Maroof M. Adil, Paola A. Lopez, David V. Schaffer, and Thomas Gaj

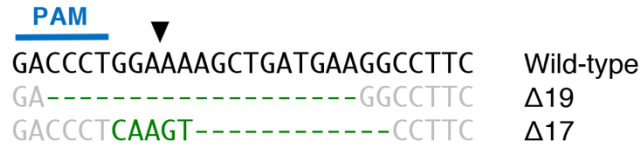


Figure S1. Sanger sequencing of individual HTT transgenes. Human HTT transgenes from the HTT-CFP reporter plasmid were PCR amplified from transfected HEK293T cells and cloned into pcDNA 3.1 for Sanger sequencing. Indels are colored dark green. Wild-type sequence is colored grey. Arrowhead indicates the predicted SaCas9 cleavage site.

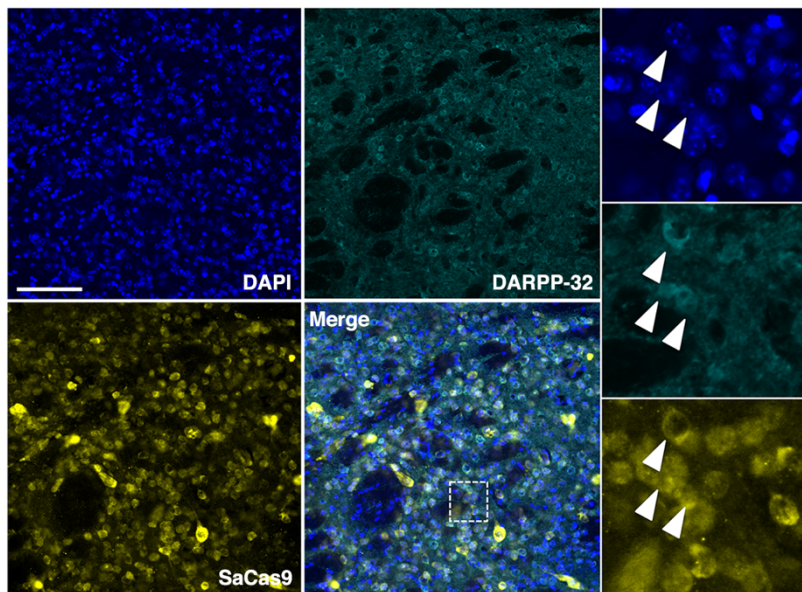


Figure S2. AAV1 can mediate delivery of CRISPR-Cas9 to the striatum. Immunofluorescent staining of striatal sections four weeks after R6/2 mice were injected with 6×10^{10} vector genomes of AAV1-SaCas9-HTT or AAV1-SaCas9-mRosa26. Arrowheads indicate representative SaCas9⁺ and DARPP-32⁺ cells. Inset showed high-magnification image. Scale bar, 100 μ m.

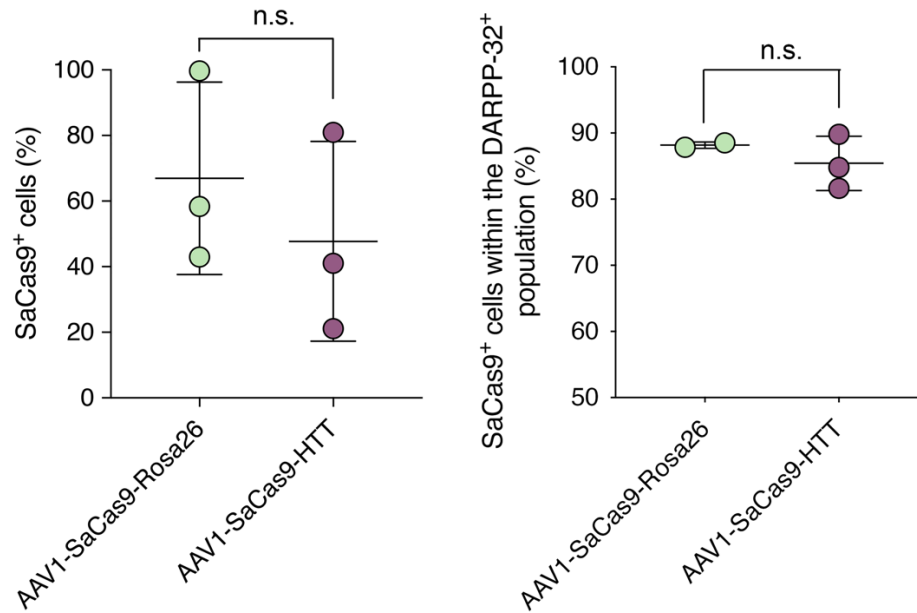


Figure S3. Quantitation of SaCas9 expression in the striatum. Mean number of (left) SaCas9⁺ and (right) dual SaCas9⁺ cells within the DARPP-32⁺ cell population in the striatum four weeks after R6/2 mice were injected with 6×10^{10} vector genomes of AAV1-SaCas9-HTT ($n = 3$) or AAV1-SaCas9-mRosa26 ($n = 3$). Circles represent data from an injected hemisphere. Error bars indicate SD. n.s. indicates not-significant, unpaired t test.

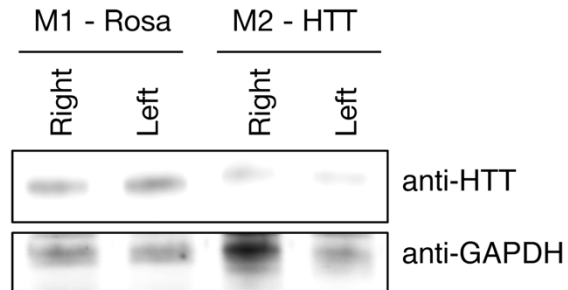


Figure S4. CRISPR-Cas9-mediated gene editing reduced mutant HTT protein in R6/2 mice.

Representative western blot of striatal lysate from two R6/2 mice four weeks after a bilateral injection with 6×10^{10} vector genomes of (left) AAV1-SaCas9-mRosa26 or (right) AAV1-SaCas9-HTT. “Left” and “right” denotes the injected hemisphere. Quantitation of western blot results in Fig. 2E.



Figure S5. CRISPR-Cas9 induces indels in the human HTT gene *in vivo*. (A) Representative indels from the human HTT transgene from homogenized striatal tissue harvested from R6/2 mice at 8 weeks following stereotaxic injection with 6×10^{10} vector genomes of AAV1-SaCas9-HTT. Indels are colored dark green. Wild-type sequence is colored grey. Arrowhead indicates predicted SaCas9 cleavage site. The binding site for 3' next-generation sequencing (NGS) primer used for PCR amplification is indicated in light green. (B) Indel frequencies from NGS analysis from mice treated with 6×10^{10} vector genomes of either AAV1-SaCas9-mRosa26 or AAV1-SaCas9-HTT. Indels were quantified using CRISPResso within a 25 bp window around the predicted cleavage site (base substitutions were ignored).

A

hHTT	GAAGGCCTTCATCAGCTTTTC	
mHTT	GAAGGCCTTCATCAGCTTTTC	Chr 5:34761912
OT1	GAAGGgCTaCATCAGCTTGCTTC	Chr 7:93570016
OT2	G--GGCCTTCAaCAGCTTTTC	Chr 3:10135241
OT3	GAAGGC-TTCATaAGCTgTTC	Chr 3:41559057
OT4	GAAGG--TTaATaAGCTTTTC	Chr 3:69106284
OT5	GAAGGgCTTCAT--GgTTTTTC	Chr 3:25571752
OT6	GAAGaCCTTC--CAGCTTTTg	Chr 7:74116528
OT7	GAAGGgCT-CATCAGCTTTcC	Chr 1:124841961
OT8	GAAGGaCTTCAT--GCTgTTC	Chr 6:73244101
OT9	GgAGtCCT--ATCAGCTTTTC	Chr 19:57577634

B

	AAV9-SaCas9-HTT	AAV9-SaCas9-mRosa26
mHTT	0.12% ± 0.01%	0.19% ± 0.05%
OT1	0.04% ± 0.01%	0.11% ± 0.08%
OT2	0.03% ± 0.01%	0.04% ± 0.01%
OT3	0.03% ± 0.01%	0.03% ± 0.01%
OT4	0.05% ± 0.02%	0.05% ± 0.02%
OT5	0.11% ± 0.01%	0.12% ± 0.01%
OT6	0.04% ± 0.02%	0.03% ± 0.02%
OT7	0.08% ± 0.03%	0.07% ± 0.02%
OT8	0.03% ± 0.01%	0.03% ± 0.01%
OT9	0.06% ± 0.02%	0.07% ± 0.01%

Figure S6. Analysis of off-target mutations introduced by CRISPR-Cas9 (A) Sequence and genomic location of the candidate off-target sites in the mm10 mouse reference genome identified using Cas-OFFinder. Target mismatches are colored red. **(B)** Indel frequencies at candidate off-target sites R6/2 mice injected with 6×10^{10} vector genomes of either AAV1-SaCas9-mRosa26 or AAV1-SaCas9-HTT. Indels were quantified within a 25 bp window around the predicted cleavage site (base substitutions were ignored).

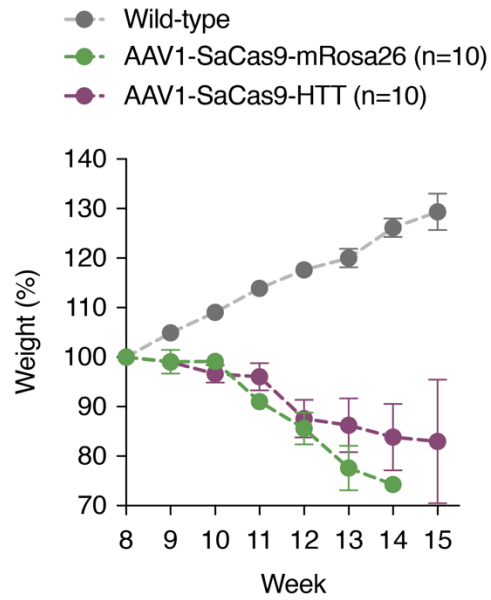


Figure S7. Genome editing did not significantly affect weight loss in R6/2 mice. Weight of R6/2 mice bilaterally injected with 6×10^{10} vector genomes of AAV1-SaCas9-HTT ($n = 10$) and AAV1-SaCas9-mRosa26 ($n = 10$). Wild-type ($n = 11$) are litter-matching B6CBAF1 mice. Values are means and error bars indicate S.E.M. Weight was analyzed using a two-way analysis of variance (ANOVA) followed by Tukey's post hoc analysis.

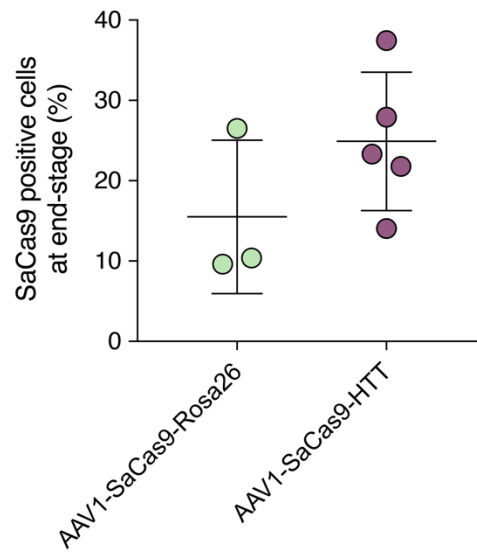


Figure S8. CRISPR-Cas9-mediated gene editing increases neuron survival. Mean number of SaCas9⁺ cells in the striatum at end-stage for R6/2 mice bilaterally injected with 6×10^{10} vector genomes of AAV1-SaCas9-HTT ($n = 3$) or AAV1-SaCas9-mRosa26 ($n = 3$). Circles represent individual mice. Error bars indicate SD. n.s. indicates not-significant, unpaired t test.

Table S1

Oligonucleotides used in this study.	
Name	Sequence (5' to 3')
hSyn-SpeI-Fwd	ATTATTGACTAGTCTGCAGAGGGCCCTGCGTATGAGTGCAAG
hSyn-AgeI-Rev	GGTGGCACCGGTCGACTGCGCTCTCAGGCACGACACGACTCC
HTT-sgRNA-1-Fwd	CACCGAAGGCCTTCATCAGCTTTTC
HTT-sgRNA-1-Rev	AAACGAAAAGCTGATGAAGGCCTTC
HTT-sgRNA-2-Fwd	CACCGCTGCTGCTGGAAGGACTTGA
HTT-sgRNA-2-Rev	AAACTCAAGTCCTTCCAGCAGCAGC
HTT-sgRNA-3-Fwd	CACCGCAGCGGCTGTGCCTGCGGCG
HTT-sgRNA-3-Rev	AAACCGCCGCAGGCACAGCCGCTGC
EcoRI-HTT-Exon 1-Fwd	GGCTAGGAATTCCCGCTCAGGTTCTGCTTTTA
XbaI-HTT-Exon 1-Rev	GGCTAGTCTAGATGGAAGGACTTGAGGGACTC
qPCR-BGH-Fwd	GCCTTCTAGTTGCCAGCCAT
qPCR BGH Rev	GGCACCTTCCAGGGTCAAG

R6/2-Genotype-Fwd	CCGCTCAGGTTCTGCTTTTA
R6/2-Genotype-Rev	TGGAAGGACTTGAGGGACTC
Off Target mHTT FWD EXT	GCGGAGAGTCTTAAACTAGCAGAGG
Off Target mHTT REV EXT	TGCTGCTGCTGTTGCTGCTGAAACG
Off Target 1 FWD EXT	TATTAGTGGGTGGAGTCTGATGTGT
Off Target 1 REV EXT	TAATCTCTCAACATCAATGGCCTCA
Off Target 2 FWD EXT	GTTGGGTTTATCAGGTATGAAGACAA
Off Target 2 REV EXT	CCGCAGTATAACAATGCTGCATTA
Off Target 3 FWD EXT	ACTATGAAGCAGGGCAGAATGAAGG
Off Target 3 REV EXT	CAAATTAAGAACCATATTCTTCCACATT
Off Target 4 FWD EXT	TGTAAAGTTACATATATGTCCCCAACC
Off Target 4 REV EXT	CCAGGGATCCAACCTAAAGTCCTTAG
Off Target 5 FWD EXT	GGGTGCACATGACATTTTGTAATTTTG
Off Target 5 REV EXT	CGTGAGCTAATTGTTCTTATCACAAC

Off Target 6 FWD EXT	TCGGAGGCTTCATCAGCACTTTCTC
Off Target 6 REV EXT	CATTGAATTTAGGGTACATCCTACATCC
Off Target 7 FWD EXT	AGATATTACCAGAATACAATCTGCC
Off Target 7 REV EXT	GGTGAGTTTACAAATTTAGAAGTTTCC
Off Target 8 FWD EXT	GGTCATTGCTGACAATCTACTTCTC
Off Target 8 REV EXT	CATGTAATGTAATATCATGCTAAAGGC
Off Target 9 FWD EXT	GCTGATAACAAAATCTGGGATGGCC
Off Target 9 REV EXT	GAACTGCTACCATCTTTGAAATGTAAC
On Target hHTT FWD EXT	CCGCTCAGGTTCTGCTTTTA
On Target hHTT REV EXT	CTGCTGCTGCTGGAAGGACT
Off Target mHTT FWD INT	NNNNNGCTCTTCCGATCTTAAGTGGCGCCGCGTAG TGCCAGTA
Off Target mHTT REV INT	NNNNNGCTCTTCCGATCTTGCTGCTGCTGTTGCTGC TGAAACGACTTG
Off Target 1 FWD INT	NNNNNGCTCTTCCGATCTGAAGTGTCTTCCCCATC TCTTGATTAATT
Off Target 1 REV INT	NNNNNGCTCTTCCGATCTTACATAATCTCAGAGCA AAGGGCTGGAATA

Off Target 2 FWD INT	NNNNNGCTCTTCCGATCTCCTATCAGCCAACCTGA AGTGTCTCATTTTC
Off Target 2 REV INT	NNNNNGCTCTTCCGATCTACTCCAGCATGTGTTCTG TAATGCCAGAA
Off Target 3 FWD INT	NNNNNGCTCTTCCGATCTCTGGGTGGGCATTGTTA CTAGTCAGTCTGT
Off Target 3 REV INT	NNNNNGCTCTTCCGATCTAGGAGGAGAGATGGTAG GTTAAGGGATTGG
Off Target 4 FWD INT	NNNNNGCTCTTCCGATCTAGCCTAGCCTACATAAT AAGACTCTATCTC
Off Target 4 REV INT	NNNNNGCTCTTCCGATCTTTAAGGGAATGGATATA CAGTGCATCTGGT
Off Target 5 FWD INT	NNNNNGCTCTTCCGATCTCGCTAGATTAAGAAGCA TGTAATGGCAGC
Off Target 5 REV INT	NNNNNGCTCTTCCGATCTGGACTGTGATGAGAAAA TTAGAGGCTCTAA
Off Target 6 FWD INT	NNNNNGCTCTTCCGATCTCAAGACCCAGCGTATTG TAAAACACAAGAA
Off Target 6 REV INT	NNNNNGCTCTTCCGATCTAGTTAAGACATGGGTCT ATCATCTAGCGGA
Off Target 7 FWD INT	NNNNNGCTCTTCCGATCTACTTTCTCAAGATCTAG ACTCACACTAGAC
Off Target 7 REV INT	NNNNNGCTCTTCCGATCTGTGTTTCAATGTTTATGT GCATATATACCATGTG
Off Target 8 FWD INT	NNNNNGCTCTTCCGATCTGGGTTTTTCATAAATTCT TACATTAAGAGGGC
Off Target 8 REV INT	NNNNNGCTCTTCCGATCTACAGCCACAATGGGAGC CCCTCACA

Off Target 9 FWD INT	NNNNNGCTCTTCCGATCTCATAACTAATAGGAACA AACTGTGACTTTA
Off Target 9 REV INT	NNNNNGCTCTTCCGATCTCAAAGATCTTAGGGTTG CTGCCAAAGGACA
On Target hHTT FWD INT	NNNNNGCTCTTCCGATCTCCCATTCATTGCCCCGGT GCTGAGC
On Target hHTT REV INT	NNNNNGCTCTTCCGATCTCTGCTGCTGCTGGAAGG ACT